RSC Advances

PAPER

View Article Online
View Journal | View Issue

Cite this: *RSC Adv.*, 2023, **13**, 36382

Study on the efficiency and recyclability of Fenton-$MnFe_2O_4$ for the degumming of hemp fibers

Chunyu Yu,[a] Yongjie Zheng,*[bc] Ying Sun[bc] and Jiayi Wang[c]

Traditional alkali degumming (TAL) has been widely used for hemp degumming; however, the produced degumming waste liquid pollutes the environment. For this phenomenon, an improved Fenton oxidation degumming process was developed in this study, that is, $MnFe_2O_4$ (Fenton-$MnFe_2O_4$) was added to the Fenton system. The purpose was to reduce the reaction time and the addition of chemical reagents, and reuse the added $MnFe_2O_4$. The effects of the Fenton-$MnFe_2O_4$ system on fiber properties (such as residual gum rate, and breaking strength) and the recyclability of $MnFe_2O_4$ were studied. The results indicated that the hemp fiber could be separated by Fenton-$MnFe_2O_4$ treatment (5.30% H_2O_2 (w/w), 0.310% $FeSO_4 \cdot 7H_2O$ (w/w), 0.040% $MnFe_2O_4$ (w/w), 40.0 °C, 40.0 min). The breaking strength of the refined fiber was 18.22 cN per dtex, and the residual gum rate was 5.47%. Compared with the TAL system, the time was shorter, energy consumption was less and pollution was smaller. In addition, the fiber treated with $MnFe_2O_4$ after five cycles still showed excellent properties, namely, 15.76 cN per dtex breaking strength and 7.79% residual gum rate, which met the needs of the spinning process. Therefore, Fenton-$MnFe_2O_4$ show great development potential in hemp fiber degumming.

Received 28th October 2023
Accepted 16th November 2023

DOI: 10.1039/d3ra07352a

rsc.li/rsc-advances

Introduction

Hemp, also known as industrial hemp, is considered to be a fiber material with superior performance due to its excellent air permeability and antibacterial properties. The untreated hemp fiber has a complex chemical composition, which is composed of cellulose components and non-cellulose components, such as pectin, hemicellulose and lignin.[1] These non-cellulose components are collectively referred to as resins. The content of pectin, fat wax and other substances in the hemp fiber is not high, and lignin and hemicellulose are the focus of degumming treatment. The content of gum has a great influence on the subsequent textile processing of hemp. Therefore, in order to carry out the subsequent textile process smoothly, it is a crucial step to remove these non-cellulose resin components to obtain pure cellulose fibers.

Degumming is the process of removing resin from the phloem composite structure. At present, the degumming methods of hemp fibers are mainly divided into three kinds, namely, biological degumming, physical degumming and chemical degumming. The biological degumming method is mainly divided into microbial degumming and biological enzyme degumming. The biological degumming method has less environmental pollution; however, the reaction time is generally long and the biological enzymes are expensive. Physical degumming is the process of removing fiber gum only using mechanical processing equipment.[2] The treated fiber breakage leads to poor separation and short fiber length, and because the degumming effect is not obvious, it is usually used as a method of fiber degumming pretreatment.[3] The chemical degumming method is a relatively developed degumming method at present. The traditional alkali degumming method is one of the chemical degumming methods. It is an earlier method used in degumming; however, it requires a large amount of alkali, a long reaction time and high energy consumption and causes great environmental pollution. At present, the emerging chemical degumming methods include organic solvent degumming, electrochemical degumming, and Fenton oxidation degumming. Fenton oxidation degumming is an advanced oxidation technology, which is increasingly popular because of its high stability, high degradation rate and no secondary pollution. It can produce strong oxidative free radicals (mainly hydroxyl radical $HO^{\bullet}$), which can completely decompose organic pollutants into non-toxic substances, such as CO_2 and H_2O. In the past two decades, various advanced oxidation technologies based on $HO^{\bullet}$ generation have been widely explored and classified according to the main sources of free radicals, including catalytic wet oxidation, ozone oxidation,[4] electrochemical oxidation, Fenton/Fenton-like method, and photochemical oxidation. Among them, the Fenton/Fenton-like method is an advanced oxidation process that has been studied earlier and widely used.

[a]College of Chemistry and Chemical Engineering, Qiqihar University, China
[b]Engineering Research Center for Hemp and Product in Cold Region of Ministry of Education, Qiqihar University, China. E-mail: zyj1964@163.com
[c]College of Light Industry and Textile, Qiqihar University, No. 42 Cultural Street, Jianhua District, Qiqihar City, Heilongjiang Province, 161000, China

Fenton-$MnFe_2O_4$ is used in this work for an improved Fenton degumming method based on Fenton oxidation degumming. According to previous studies, the optimal concentration of Fenton oxidation degumming is 1% (w/w) $FeSO_4 \cdot 7H_2O$, 9% (w/w) H_2O_2, and temperature 80 °C. Compared with TAL, this reaction condition has greatly reduced energy consumption and pollution.[5] The purpose of adding $MnFe_2O_4$ to the Fenton system is to reduce the addition of H_2O_2 and $FeSO_4 \cdot 7H_2O$, and to reduce energy consumption and pollution again on the basis of the Fenton system.

Materials and methods

Materials and chemicals

The hemp fiber used in this experiment is too coarse short hemp (produced in Heilongjiang Province, China). The Fenton reagent used is 30% hydrogen peroxide (H_2O_2) and ferrous sulfate ($FeSO_4 \cdot 7H_2O$), purchased from Tianjin Kaitong Chemical Reagent Co. Ltd. Sodium hydroxide (NaOH) for traditional alkali degumming was purchased from Liaoning Quanrui Reagent Co. Ltd. $MnFe_2O_4$ for Fenton's improvement, synthesized from ethylene glycol (EG), ferric chloride ($FeCl_3 \cdot 6H_2O$), and manganese chloride ($MnCl_2 \cdot 4H_2O$) with adjusted acidity by sodium acetate (NaAc), was purchased from Tianjin Fuyu Fine Chemical Co. Ltd. The reagents used in the experiment were all of analytical grade, and deionized water was used throughout the experiment.

Preparation of $MnFe_2O_4$

The synthesis method of $MnFe_2O_4$ is as follows: first, NaAc (2.7 g) was completely dissolved in EG (30 mL) under ultrasound for 15 minutes, and the molar ratio of $MnCl_2 \cdot 4H_2O$ and $FeCl_3 \cdot 6H_2O$ was 1 : 2.[6] The mixture was then transferred to an autoclave and placed in an oven at 180 °C for 10 h. After naturally cooling down to room temperature, the autoclave was opened, the solution was transferred to the beaker, and the prepared $MnFe_2O_4$ was sucked out with a magnet. Then, it was washed three times with water and ethanol, and dried at 50 °C. Finally, dry $MnFe_2O_4$ was stored at room temperature for further use.

Traditional alkali degumming hemp fibers

In this study, the traditional alkali degumming process was used as a control group.[7] The specific experimental materials and reaction conditions are shown in Table 1. The experimental process is shown in Fig. 1. The weight of the raw hemp sample used in each degumming process was about 20.0 g, and the dosage of chemical agent was the weight percentage of the hemp fiber (w/w).[5]

Table 1 Experimental raw materials and reaction conditions of the traditional alkali degumming process

	Pickling	One alkali boil	Secondary alkali cooking
Chemical dose (w/w)%	H_2SO_4: 2	NaOH: 5 Na_2SiO_3: 2 Na_2SO_3: 2.5	NaOH: 15 Na_2SiO_3: 2.5 Na_2SO_3: 2
Temperature (°C)	50	100	100
Time (min)	60	120	180
Water bath ratio	1 : 10	1 : 10	1 : 10

Fenton degumming process of hemp

In this study, the Fenton degumming hemp process was used as a control group. The specific experimental reagents and reaction conditions are shown in Table 2. The weight of raw hemp sample used in each degumming process was about 20.0 g, and the dosage of chemical agent was the weight percentage of hemp fiber (w/w).

Fenton-$MnFe_2O_4$ degumming process

The effects of Fenton-$MnFe_2O_4$ process parameters on hemp fiber properties were studied. Different contents of $MnFe_2O_4$ (0%, 0.015%, 0.025%, 0.035%, and 0.045%, (w/w)), different contents of H_2O_2 (0%, 4%, 5%, 6%, and 7%, (w/w)) and different contents of $FeSO_4 \cdot 7H_2O$ (0%, 0.1%, 0.25%, 0.40%, and 0.55%) were added into the Fenton solution to form the degumming solution, and 20 g raw hemp was immersed in the solution at 40 °C for 40 min.[7] The degummed fiber was washed with deionized water to remove the glial residues, impurities and chemical reagents on the surface of the fiber. Finally, it was dried in an oven to obtain a refined dry hemp.[8]

On the basis of the primary single-factor experiment, three important variables, namely, $FeSO_4 \cdot 7H_2O$ content, H_2O_2 content and $MnFe_2O_4$ content, were optimized. By using the Box–Behnken Design (BBD) called the response surface method (RSM), the correlation between the single factor effect of factors and indexes and the interaction between factors was studied. In this study, a three-factor three-level design was used, and 17 experiments were needed. The $FeSO_4 \cdot 7H_2O$ content (X_1), H_2O_2 content (X_2), $MnFe_2O_4$ content (X_3) and residual gum content (Y_1) were evaluated.

Determination of the residual gum content (RGC) of hemp fibers

The residual gum content and chemical composition content were analyzed according to GB/T5889-1986.[9] The residual glue ratio was calculated as shown in eqn (1):

$$\mathrm{RGC} = \frac{W_0 - W_1}{W_0} \times 100\% \quad (1)$$

where W_0 is the dry weight of the industrial hemp fiber before treatment expressed in g and W_1 is the dry weight of the industrial hemp fiber after treatment expressed in g.

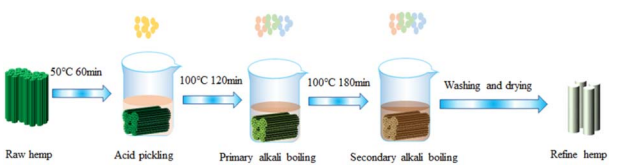

Fig. 1 Traditional alkali degumming process.

Table 2 Experimental raw materials and reaction conditions of the Fenton degumming hemp process

	Oxidation	Reduction	Soda boiling
Chemical dose (w/w)%	H_2O_2: 6 $FeSO_4 \cdot 7H_2O$: 1 Anthraquinoe: 1.5 NaOH: 7.0	$NaHSO_3$: 5	NaOH: 7
pH	4		
Temperature (°C)	50	90	100
Time (min)	90	60	90
Water bath ratio	1 : 15	1 : 10	1 : 10

Fourier transform infrared (FT-IR) spectroscopic analysis

By Fourier transform infrared spectroscopy, a certain amount of industrial hemp fiber and KBr were mixed and ground, and then pressed into thin slices. The structure was characterized. The scanning range was 4000–500 cm^{-1}, the resolution was 4 cm^{-1}, and each wavelength was scanned 32 times.[10]

Thermogravimetric analysis

A STA449F3 synchronous thermal analyzer was used to analyze the thermal stability of the industrial hemp fiber before and after degumming.[11] The test was conducted in a nitrogen atmosphere at a gas flow rate of 10 mL min^{-1}. The test range was from 25 °C to 600 °C at a heating rate of 10 °C min^{-1}.

Scanning electron microscopic (SEM) analysis test

A scanning electron microscope (SEM) was used to observe the surface morphology of the industrial hemp fiber before and after degassing by adjusting different multiples of a S-3400 scanning electron microscope.[12]

Fracture strength test

The fracture strength test was analyzed according to GB/T5889-1986. The test was conducted using a LY-06E electronic single fiber strength meter, with a tensile interval of 10 mm and a tensile rate of 20 mm min^{-1}. The tensile times of each sample were 20 times, and the average value was taken.

Polymerization degree test

The polymerization degree of hemp fiber was tested using the Chinese standard GB/T5888-86.[13] First, the hemp fiber was defatted in a fat extractor with a mixture of benzene and ethanol in a ratio of 2/1 (v/v), and the sample was chopped into fragments (≤1 mm). The hemp sample was then dissolved in a copper–ethylenediamine solvent.[10] The contents of ethylenediamine and copper in a solvent were 2.03 and 0.99 mol L^{-1}, respectively. A viscosimeter was used to measure the viscosity of hemp samples.

X-ray diffraction analysis (XRD)

The crystal structure and crystallinity analysis of the hemp fiber was performed using a wide-angle X-ray diffractometer equipped with a CuKa radiation source (40 kV/180 mA).[14] X-ray diffraction (XRD) patterns were recorded at a scan rate of 2° min^{-1} over a 2 hour period, ranging from 5 to 50°.

Acid group content test

The aldehyde (–CHO) and carboxylic (–COOH) contents of the hemp fiber were measured by conductivity titration. First, 0.3 grams of dried fiber sample was placed in water (55 mL) and 0.01 M sodium chloride solution (5 mL). The mixture was stirred, so that it becomes a fully dispersed suspension. Then, 0.1 M hydrochloric acid was added to this mixture to adjust the pH at 2.5–3.0. Finally, 0.04 M NaOH solution was added at a rate of 0.1 mL min^{-1} and the pH was adjusted to 11.

Results and discussion

Reaction mechanism of Fenton-$MnFe_2O_4$ degumming

The Fenton oxidation method is a kind of oxidative degumming process. The Fenton reagent is a combination of hydrogen peroxide and iron catalyst, which is used to destroy organic compounds or oxidize pollutants in industrial wastewater. Ferrous sulfate is usually used as a catalyst.[5] As shown in reaction eqn (2)–(5), H_2O_2 can convert Fe^{2+} into Fe^{3+}, and H_2O_2 is decomposed into $OH^{\bullet}$ and OH^- in this process; H_2O_2 reduced Fe^{3+} to Fe^{2+}, and H_2O_2 was decomposed into $HOO^{\bullet}$ and H^+. The net effect is the disproportionation of hydrogen peroxide to produce two different oxygen free radicals, and water (H^+ + OH^-) is a by-product.[15] Compared with other methods, the Fenton oxidation degumming method has the advantages of fast reaction time and low energy consumption, but it still causes some pollution to the environment. Therefore, we consider adding $MnFe_2O_4$ to the Fenton system, a catalyst that can promote the decomposition of H_2O_2 and degrade the degumming waste liquid, so as to reduce the addition of H_2O_2 in the Fenton system and reduce the chemical oxygen demand (COD) value of the degumming waste liquid. Moreover, $MnFe_2O_4$ is magnetic and can be reused more than 5 times, which greatly reduces the cost of degumming.

$$Fe^{2+} + H_2O_2 = Fe^{3+} + OH^- + HO^{\bullet} \quad (2)$$

$$Fe^{3+} + H_2O_2 + OH^- = Fe^{2+} + H_2O + HO^{\bullet} \quad (3)$$

$$Fe^{3+} + H_2O_2 = Fe^{2+} + H^+ + H_2O^{\bullet} \quad (4)$$

$$H_2O^{\bullet} + H_2O_2 = H_2O + O_2\uparrow + HO^{\bullet} \quad (5)$$

As shown in chemical formula (2)–(5), in the process of hemp degumming, various free radicals including $HO^{\bullet}$ and $HOO^{\bullet}$ are produced during the Fenton oxidation process, and Fe^{2+} and Fe^{3+} can be converted to each other. The main reason why Fenton's reagent has catalytic degradation ability for many organic compounds is the presence of $H^{\bullet}$ and $HOO^{\bullet}$ with high oxidation potential.[16] $H^{\bullet}$ and $HOO^{\bullet}$ free radicals oxidize the gum of hemp to break it into small molecules. The gum is mainly composed of hemicellulose, lignin and cellulose. Hemicellulose is closely linked to lignin through covalent

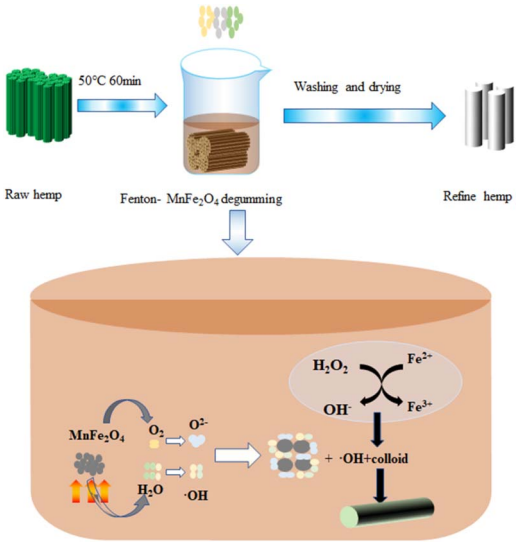

Fig. 2 Fenton-$MnFe_2O_4$ degumming process and reaction mechanism.

bonds, thus causing the most important interaction between lignin and cellulose, and endowing lignin–hemicellulose–cellulose with a network rigid structure. In addition, the decomposition of hemicellulose, lignin and other carbohydrates can trigger each other.[14] At the same time, due to the supramolecular structure of cellulose, it is difficult to decompose cellulose.

The hydroxyl groups formed by the Fenton reaction can oxidize the hydroxyl groups of cellulose and form new carboxyl groups on the cellulose chain. The carboxyl content increased with the increase in hydrogen peroxide consumption.[17] When the C2 and C3-hydroxyl groups of the glucose group on the cellulose chain are oxidized to carboxyl groups, the DP of the cellulose macromolecules decreases sharply.[16] Due to the non-selective oxidation of cellulose by the Fenton reagent, the oxidative degradation of the 1,4-β-D-glucoside bond of the cellulose chain is reduced. The above-mentioned effects destroy the network structure of the microfibers that form the fiber cell wall, resulting in the weakening of the fiber structure and the destruction of the rigid structure of the lignin–hemicellulose–cellulose network. As shown in Fig. 3(a), it shows the change in fiber polymerization degree under different treatment methods,

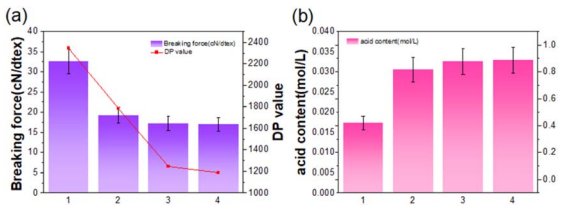

Fig. 3 (a) Polymerization degree and breaking strength of the hemp fiber. (b) Acid group content of the hemp fibre. Among them, 1 is raw hemp, 2 is traditional alkali degumming, 3 is Fenton degumming, and 4 is Fenton-$MnFe_2O_4$ degumming.

and the decrease in fiber polymerization degree can also be observed. At the same time, the fiber breaking strength and the degree of polymerization of the fiber change in the same trend also showed a downward trend, which also confirmed that the network rigid structure of the fiber was destroyed. Therefore, the gum on the surface of the hemp fiber is gradually decomposed into small molecules. Dissolved in the degumming solution, the degumming solution changes from the original brown to yellow with the change in reaction time. This color change may be that the degumming solution in the solution reacts completely, and the ferrous ion is oxidized to the iron ion, and the color of the iron ion in the aqueous solution may also indicate that the degumming solution dissolves cellulose. The degumming solution used in the traditional alkali degumming method is dark brown, and the color of the degumming solution of the Fenton system becomes lighter, which may be due to the hydroxyl radical (HO$^{\bullet}$) and hydrogen peroxide radical (HOO$^{\bullet}$) produced by the catalytic hydrogen peroxide of ferrous ions. The color of the Fenton-$MnFe_2O_4$ degumming solution is darker than that of the Fenton degumming solution. This is because the color of $MnFe_2O_4$ is darker, generally dark brown or black, which will affect the color change of the degumming solution and make it darker. Therefore, in the preliminary preparation process, it is necessary to pay attention to the amount of Mn and Fe added in the synthesis of $MnFe_2O_4$. In addition, in the experiment, we also found that the pH of the degumming solution will increase, because hydroxyl radicals, as a strong oxidant (E_0 = 2.8 V), can cause the degradation of polysaccharides and produce acidic groups. As shown in Fig. 3(b), the amounts of acidic groups of the hemp fiber treated in different ways are different, which reflects the degree of oxidative decomposition of the hemp fiber to a certain extent. As a strong oxidant (E_0 = 2.8 V), HO$^{\bullet}$ can cause the degradation of polysaccharides.[16,18] At a certain pH, the Fenton process can effectively degrade dissolved or colloidal organic matter in wastewater, making the color of the solution change from dark brown to yellow (Fig. 4).

Manganese ferrite is a kind of peroxidase-like enzyme. When manganese ferrite is excited, an electron and a hole are generated. The electron interacts with trace O_2 in the degumming solution to form superoxide anion O^{2-}, while the hole interacts with H_2O molecules to form HO$^{\bullet}$ free radicals.[19] The generated O^{2-} and HO$^{\bullet}$ can directly react with the colloid and wastewater pollutant molecules adsorbed on the surface of the ferrite, thereby catalyzing hydrogen peroxide in the Fenton system, enhancing the activity of the Fenton system, degumming and

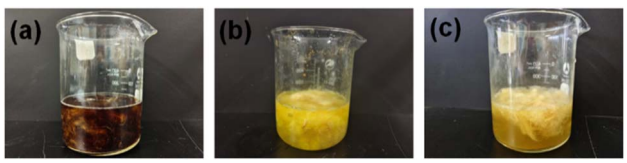

Fig. 4 Color of the degumming solution with different treatment methods: (a) traditional alkali degumming, (b) Fenton degumming, and (c) Fenton-$MnFe_2O_4$ degumming.

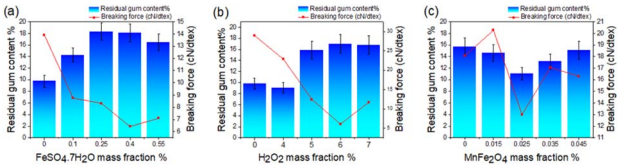

Fig. 5 Influence of the Fenton-$MnFe_2O_4$ process on degumming effects. (a) Influence of the addition amount of $FeSO_4{\cdot}7H_2O$ on degumming effects. (b) Influence of the addition amount of H_2O_2 on degumming effects. (c) Influence of the addition amount of $MnFe_2O_4$ on degumming effects.

degrading the pollutants of the degumming solution. The possible reaction mechanism is shown in Fig. 2.

Effect of the Fenton-$MnFe_2O_4$ system addition on degumming effects

Effect of the Fenton-$MnFe_2O_4$ process on degumming effects

Effect of $FeSO_4{\cdot}7H_2O$ addition on degumming effects. As a substance that activates H_2O_2 in the Fenton system, $FeSO_4{\cdot}7H_2O$ plays a vital role in the Fenton system. Too much $FeSO_4{\cdot}7H_2O$ will cause the Fenton system to produce too much iron mud, causing environmental pollution. Too little $FeSO_4{\cdot}7H_2O$ will cause the Fenton system to react incompletely and the hemp degumming is not thorough enough. Therefore, we studied the effect of 0–0.55% (w/w) $FeSO_4{\cdot}7H_2O$ content on the degumming effect. As shown in Fig. 5(a), the breaking strength of the fiber first decreases and then increases with the increase in $FeSO_4{\cdot}7H_2O$ concentration, and the residual gum rate first decreases and then increases with the increase in $FeSO_4{\cdot}7H_2O$ concentration.[20,21] The slope of fiber breaking strength and residual gum rate in the range of 0–0.1% (w/w) of $FeSO_4{\cdot}7H_2O$ concentration is large, which fully illustrates the activation effect of Fe^{2+} on H_2O_2. When the concentration of $FeSO_4{\cdot}7H_2O$ was 0.10–0.40% (w/w), the breaking strength of the fiber continued to decline, and the residual gum rate continued to rise. This may be that when the concentration of Fe^{2+} in the degumming solution was low, the hydroxyl radical $HO^{\bullet}$ produced by hydrogen peroxide was less, and the removal of the fiber gum was not complete. When the concentration of Fe^{2+} in the degumming solution was high, the activation rate of hydrogen peroxide was accelerated, the fiber gum was too high, and the original toughness was lost. When the concentration of Fe^{2+} in the degumming solution is very high, the activation rate of hydrogen peroxide is very fast, and a part of hydrogen peroxide is consumed before it can react with the gum in the fiber. This may be the reason why the fiber breaking strength increases and the residual gum rate decreases when the concentration of $FeSO_4{\cdot}7H_2O$ is in the range of 0.40–0.55% (w/w).[22]

Effect of the amount of H_2O_2 added on the degumming effect. As a component of the Fenton-$MnFe_2O_4$ system, H_2O_2 is the main substance that produces $HO^{\bullet}$ in the Fenton-$MnFe_2O_4$ system. The amount of H_2O_2 added to a certain extent reflects how much $HO^{\bullet}$ is produced and determines the degree of oxidation of the system. Therefore, we studied the effect of 0–7.0% (w/w) H_2O_2 concentration on the degumming effect. As shown in Fig. 5(b), in the range of 0–7.0% (w/w) H_2O_2 concentration, the breaking strength of the fiber first decreased and then increased, and the residual gum first decreased, then increased and then decreased.[23] It can be seen that the concentration of H_2O_2 has a great influence on the degumming of hemp. The breaking strength of the hemp fiber decreased in the range of H_2O_2 concentration of 0–6.0% (w/w),[24] which may be due to the increase in the activated group $HO^{\bullet}$ with the increase in H_2O_2 concentration, and the degree of oxidation of the gum of the hemp fiber also increased, which resulted in a decrease in the breaking strength of the hemp fiber.[25] When the concentration of H_2O_2 increases to a certain concentration, the hemp gum is completely oxidized, which leads to a continuous decrease in the breaking strength of the hemp fiber. However, when the concentration of H_2O_2 exceeds 6%, excessive $HO^{\bullet}$ will be produced.[18] These $HO^{\bullet}$ are consumed before they react with the gum in hemp, resulting in an increase in the breaking strength of 6–7% (w/w) and a small decrease in the residual gum rate.[9]

Effect of $MnFe_2O_4$ addition on degumming effects. The activation effect of $MnFe_2O_4$ on the Fenton system was further studied. We studied the effect of 0–0.045% (w/w) $MnFe_2O_4$ content on the degumming effect. As shown in Fig. 5(c), the hemp fiber breaking strength first increased and then decreased, then increased and then decreased, and the residual gum first decreased and then increased. In the range of 0–0.015% (w/w) of $MnFe_2O_4$, there are changes respectively, which show the activation effect of $MnFe_2O_4$ on the Fenton system. In the range of 0–0.025% (w/w) of $MnFe_2O_4$, the residual gum rate of the hemp fiber decreases continuously, and the slope of the change in the residual gum rate of the hemp fiber in the second section is larger than that in the first section.[26] This may be because the catalytic effect of $MnFe_2O_4$ on the Fenton system is not strong, and the content of $MnFe_2O_4$ in the second section increases, which strengthens the catalytic effect of the Fenton system and has a good degumming effect.[27] In the concentration range of 0.025–0.045% (w/w) of $MnFe_2O_4$, the residual gum rate continues to rise, which may be due to the activation of hydrogen peroxide in the Fenton system under the activation of $MnFe_2O_4$.[28] The activation speed is too fast and the reaction is consumed before it is too late. In the whole range of 0–0.045% (w/w) of $MnFe_2O_4$, the change in the breaking strength of hemp fibers is very unstable, and there is no stable trend. In the range of 0.015–0.030% (w/w) of $MnFe_2O_4$, the change in the fiber breaking strength is particularly large. This shows that $MnFe_2O_4$ has a great influence on the breaking strength of the hemp fiber.

$FeSO_4{\cdot}7H_2O$ content, H_2O_2 content and $MnFe_2O_4$ content in Fenton-$MnFe_2O_4$

In the above study, we analyzed the effects of various factors on the fiber properties in the Fenton-$MnFe_2O_4$ system. Therefore, through preliminary single-factor experiments, the range of significant changes in $FeSO_4{\cdot}7H_2O$ content (A), H_2O_2 content (B) and $MnFe_2O_4$ content (C) was determined to be 0.1–0.4%, 3–6%, 0.01–0.04%, respectively, as shown in Table 3. The Box–

Table 3 BBD factor level test and coding

Coded value	$FeSO_4 \cdot 7H_2O$%	H_2O_2%	$MnFe_2O_4$%
−1	0.10	3.0	0.010
0	0.25	4.5	0.025
1	0.40	6.0	0.045

Behnken Design (BBD) of the software Design Expert 13 response surface method (RSM) was used to study their interaction and the optimization of degumming process conditions. As shown in Table 4, the two properties of residual gum rate (Y_1) and breaking strength (Y_2) of the hemp fiber directly determine the spinnability of subsequent processing of hemp fibers, so we use these two as indicators to evaluate the fiber properties.[29]

Tables 5 and 6 are the test results of the response surface test design scheme. The results indicated that the experimental model designed according to Design Expert 13 is significant, indicating that the residual gum rate of the hemp fiber has a good fitting degree with the three factors studied. The regression effect is significant and statistically significant. According to the F value and P value, it can be concluded that in the single-factor experiment, the influence on the residual gum rate follows the order $B > A > C$, and the influence on the hemp fiber breaking strength follows the order $B > A > C$, both of which show the same trend. The effect of interaction between factors on the residual gum rate follows the order $AC > AB > BC$, and the effect of interaction between factors on breaking strength follows the order $AB > AC > BC$. The two do not show the same trend, which indicates that the effect of interaction between factors on the residual gum rate and breaking strength is no longer consistent, and there is interaction between factors. Based on the principle of least square method, the experimental data were regressed and fitted, and the quadratic function relationship Y_1 of the response surface of the residual gum rate and the quadratic function relationship Y_2 of the response surface of the breaking strength were obtained.

$$Y_1 = 52.13884 - 37.99722A - 13.83817B - 120.88889C - 1.32222AB + 233.33333AC + 17.55556BC + 57.54444A^2 + 1.26656B^2 - 1212.22222C^2 \quad (6)$$

$$Y_2 = 80.11000 - 51.7611A - 18.41333B - 177.72222C - 5.77778AB + 382.22222AC + 11.11111BC + 103.77778A^2 + 1.75778B^2 - 666.66667C^2 \quad (7)$$

Table 4 BBD experimental design table

	Coded variable level			Actual variable levels				
Run	X_1	X_2	X_3	X_1	X_2	X_3	Y_1	Y_2
1	0	0	0	0.25	4.5	0.025	8.45	20.16
2	−1	0	−1	0.1	4.5	0.01	10.79	24.47
3	1	0	−1	0.4	4.5	0.01	8.04	19.53
4	−1	0	0	0.1	3	0.025	16.96	32.14
5	0	1	1	0.25	6	0.04	6.43	15.82
6	0	0	0	0.25	4.5	0.025	7.61	18.31
7	0	−1	1	0.25	3	0.04	12.86	27.49
8	0	0	0	0.25	4.5	0.025	7.32	17.47
9	0	−1	−1	0.25	3	0.01	15.07	29.63
10	1	1	0	0.4	6	0.025	6.29	15.18
11	1	0	1	0.4	4.5	0.04	7.86	18.96
12	1	−1	0	0.4	3	0.025	13.65	28.17
13	0	0	0	0.25	4.5	0.025	7.47	17.94
14	−1	0	1	0.1	4.5	0.04	8.51	20.46
15	−1	1	0	0.1	6	0.025	10.79	24.35
16	0	0	0	0.25	4.5	0.025	8.04	19.47
17	0	1	−1	0.25	6	0.01	7.09	16.96

Fig. 6 shows the 3D response surface diagram of the interaction between the residual gum rate and the breaking strength factor. The interaction between the factors of residual gum rate is shown in Fig. 6(a)–(c). With the increase in reactant concentration, ignoring the influence of other variables, the RGC of the hemp fiber decreases rapidly to the lowest point, which indicates that the three substances of A, B and C can promote the degumming of the hemp fiber. After reaching the lowest point, there is an upward trend or it tends to be flat. This shows that it is not the higher the concentration of A, B and C, the smaller the residual gum rate of the fiber.[26] The possible reason is that with the increase in A, B and C concentration, a large number of non-cellulose components of the fiber are removed, which promotes the depolymerization of cellulose. However, when the concentration of A, B and C reaches a certain level, the reaction rate of the system becomes too fast. The substances A, B and C cannot react with the fiber colloid, but they react with other substances in the degumming solution. A, B and C cannot be used at the highest level, so that the fiber degumming is not complete, which leads to the rise after the lowest point in the response surface image. The interaction between the breaking strength factors is shown in Fig. 6(d)–(f). With the increase in the concentration of the reactant, ignoring the influence of other variables, the change in the breaking strength of the fiber decreases rapidly with the increase in the concentration of the reactant, reaching the lowest point. This shows that the three factors of A, B and C have a significant effect on the breaking strength of the fiber. After reaching the lowest point, there is a slight upward trend. This part of the upward trend may be affected by the change in the trend of fiber residual gum rate. The increase in fiber residual gum rate represents the increase of gum wrapped on the fiber surface. The increase of gum will increase the toughness of the fiber and affect the residual gum rate. High residual gum rate is often accompanied by high breaking strength. In addition, the optimal Fenton-$MnFe_2O_4$ conditions for hemp fiber RGC were obtained using the Design-Expert. 13 software, which are as follows: $FeSO_4 \cdot 7H_2O = 0.31\%$, $H_2O_2 = 5.4\%$, and $MnFe_2O_4 = 0.040\%$. Under the optimal process conditions, five parallel experiments were carried out (as shown in Table 7). The average RGC of the fiber was 5.92% ± 0.10, and the average breaking strength was 15.22 cN ± 0.10, which was close to the predicted residual gum rate of 5.79% using BBD. The breaking strength is 15.20 cN. This result

Table 5 Residual gum rate response surface regression model analysis of variance table

Source	Sum of squares	df	Mean square	*F*-Value	*p*-Value	Significant
Model	161.96	9	18.00	37.03	<0.0001	***
A-A	15.71	1	15.71	32.32	0.0007	**
B-B	97.58	1	97.58	200.79	<0.0001	***
C-C	3.55	1	3.55	7.31	0.0305	**
AB	0.3540	1	0.3540	0.7285	0.4216	
AC	1.10	1	1.10	2.27	0.1757	
BC	0.6006	1	0.6006	1.24	0.3030	
A^2	7.02	1	7.02	14.44	0.0067	**
B^2	34.28	1	34.28	70.55	<0.0001	***
C^2	0.3047	1	0.3047	0.6269	0.4545	
Residual	3.40	7	0.4860			
Lack of fit	2.55	3	0.8496	3.98	0.1075	
Pure error	0.8531	4	0.2133			

indicates that the model is predictive and reliable for the RGC of the hemp fiber.

Surface morphology analysis (SEM)

Scanning electron microscopy (SEM) was used to analyze the surface morphology of untreated hemp fibers[30] (Fig. 7(a)), traditional alkali degumming-treated hemp fibers (Fig. 7(b)), traditional Fenton degumming-treated hemp fibers (Fig. 7(c)), and Fenton-$MnFe_2O_4$ degumming-treated hemp fibers (Fig. 7(d)).

The untreated hemp fiber is rough, and the surface of the fiber is wrapped with a large amount of gum. The single fiber is adhered together by the gum to form a bundle fiber, and the single fiber is not observed[31] (Fig. 7(a)). Hemp fiber after traditional alkali degumming treatment, bundle fiber have been separated, a large number of gum on the surface of hemp fiber has been removed, but there are still some gums (Fig. 7(b)). The gum on the surface of hemp fibers treated by traditional Fenton degumming is almost removed, and the single fiber can be clearly observed. The surface of the hemp fiber is smooth. The hemp fiber treated under this condition has a small enough diameter, high dispersion and softness[26,32] (Fig. 7(c)). The raw hemp treated by the Fenton-$MnFe_2O_4$ degumming method (Fig. 7(d)) has been separated from the fiber that was originally stuck together by the gum. The single fiber is clearly visible, and the gum on the surface of the fiber has almost been removed, which is similar to the SEM image of Fig. 7(c), but the addition of H_2O_2 content is greatly reduced, which also proves the catalytic effect of $MnFe_2O_4$ on the Fenton system.

Fourier transform infrared (FT-IR) analysis

In order to verify the changes in the chemical structure of hemp fiber prepared by different methods,[25] we performed the Fourier transform infrared (FT-IR) analysis, as shown in Fig. 8(a). The –OH stretching vibration at about 3148 cm^{-1}, the C–H stretching vibration at about 2916 cm^{-1}, the cellulose β-1,4-glycosidic bond at 899 cm^{-1}, and the C–OH stretching vibration at 668 cm^{-1} are the characteristic peaks of the infrared spectrum of cellulose. These peaks exist in all four groups of samples, indicating that the main component of hemp fiber is cellulose. After the treatment of hemp fiber, the intensity of these peaks increased, indicating that the non-cellulose components in the hemp fiber were removed and the cellulose components of hemp fiber were improved.[29] The C=O stretching at about 1733 cm^{-1} is derived from ketones or esters in hemicellulose. This peak only exists in raw hemp, and other treated hemp fibers do not have this peak, indicating that hemicellulose in hemp fiber gum is more easily oxidized and decomposed. The vibration of the acidic group (carboxyl or aldehyde group) of the hemp fiber at about 1640 cm^{-1} can be observed.[33] The strength of the place is stronger than that of the raw hemp fiber,

Table 6 Response surface regression model of breaking strength analysis of variance table

Source	Sum of squares	df	Mean square	*F*-Value	*p*-Value	Significant
Model	413.43	9	45.94	26.00	0.0001	***
A-A	47.92	1	47.92	27.12	0.0012	**
B-B	254.48	1	254.48	144.01	<0.0001	***
C-C	7.72	1	7.72	4.37	0.0749	*
AB	6.76	1	6.76	3.83	0.0914	
AC	2.96	1	2.96	1.67	0.2367	
BC	0.2500	1	0.2500	0.1415	0.7180	
A^2	22.96	1	22.96	12.99	0.0087	**
B^2	65.86	1	65.86	37.27	0.0005	**
C^2	0.0947	1	0.0947	0.0536	0.8235	
Residual	12.37	7	1.77			
Lack of fit	7.41	3	2.47	1.99	0.2578	
Pure error	4.96	4	1.24			

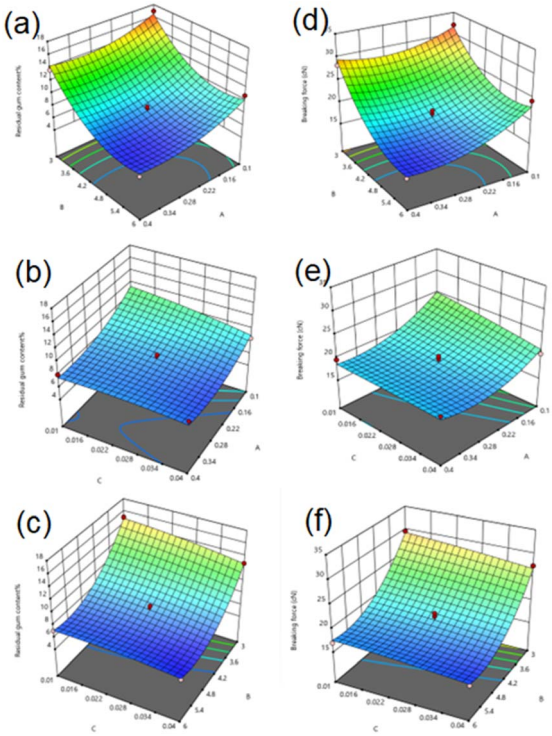

Fig. 6 Effect of interaction between factors on the residual gum rate response surface analysis. The interaction between the factors of residual gum rate is shown in (a)–(c), where (a) is the response surface curve of AB factor, (b) is the response surface curve of AC factor, and (c) is the response surface curve of BC factor. The interaction between the breaking strength factors is shown in (d)–(f), where (d) is the response surface curve of AB factor, (e) is the response surface curve of AC factor, and (f) is the response surface curve of BC factor.

especially the hemp fiber after Fenton-$MnFe_2O_4$ degumming, which indicates that more hydroxyl groups are oxidized and form carboxyl or aldehyde groups on the cellulose. This is consistent with the results in Fig. 3(b).

X-ray diffraction analysis (XRD)

Fig. 8(b) shows the X-ray diffraction patterns treated by different methods. As shown in these four curves, three main crystal peaks can be seen at $2\theta = 14.8°$, 17.0°, and 22.7°, corresponding to the 101 crystal plane, 110 crystal plane and 200 crystal plane of cellulose I, respectively.[9] This shows that for Fenton-$MnFe_2O_4$, like other degumming methods, the crystal structure and crystal type of cellulose have not changed. In addition, the peak intensity of the 200 crystal plane of cellulose I increased after Fenton-$MnFe_2O_4$ degumming treatment, indicating an increase in crystallinity.[34] The dissolution of some amorphous cellulose and hemicellulose in the hemp fiber gum will cause an increase in the crystallinity of the fiber. The traditional Fenton

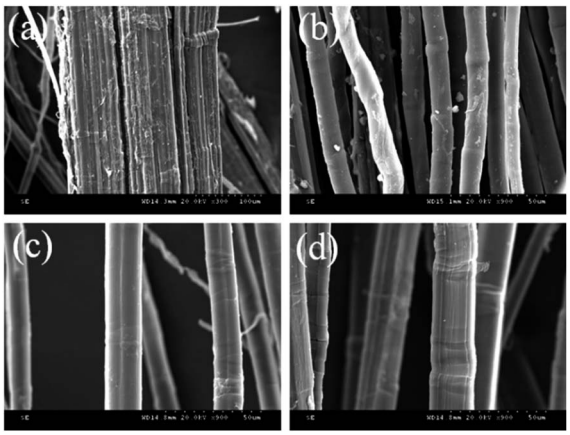

Fig. 7 SEM image of the hemp fiber: (a) untreated hemp fiber, (b) traditional alkali degumming hemp fiber, (c) traditional Fenton degumming hemp fiber, and (d) Fenton-$MnFe_2O_4$ degumming hemp fiber.

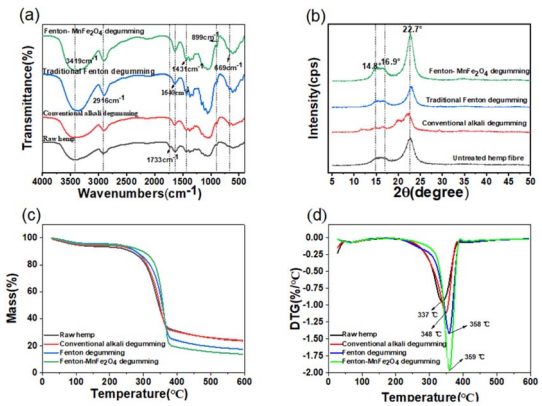

Fig. 8 Comparison of the degumming properties of hemp fibers treated by different processes: (a) FTIR spectra of the hemp fiber treated by different processes; (b) XRD patterns of the hemp fiber treated by different processes; (c) TG diagram of the hemp fiber treated by different processes; (d) DTG diagram of the hemp fiber treated by different processes.

degumming method shows the same trend of crystallinity, which also shows this. However, the crystallinity of traditional alkali degumming is reduced, because under alkaline conditions, the cellulose chain on the crystal is easier to be removed, which will result in a decrease in the crystallinity of hemp fibers.

TG and DTG analysis

In order to verify the thermal stability of hemp fibers treated by different degumming methods, we carried out TG and DTG analyses, as shown in Fig. 8(c) and (d). It can be seen from the

Table 7 Residual gum rate and breaking strength under parallel experiments

Number of parallels	1	2	3	4	5	Mean value
RGC (%)	5.87	5.98	5.96	5.84	5.94	5.92
Breaking strength (cN per dtex)	15.14	15.26	15.19	15.24	15.27	15.22

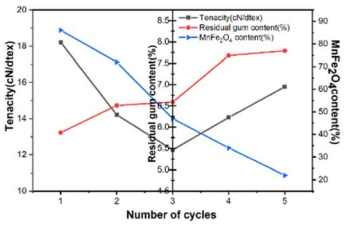

Fig. 9 Effect of $MnFe_2O_4$ cycles on the breaking strength and residue ratio of hemp fibers: (1) the $MnFe_2O_4$ hemp fiber of the first cycle; (2) the $MnFe_2O_4$ hemp fiber of the second cycle; (3) the third cycle of $MnFe_2O_4$ hemp fiber; (4) the fourth cycle of the $MnFe_2O_4$ hemp fiber; and (5) the fifth cycle of the $MnFe_2O_4$ hemp fiber.

Table 8 Content of Mn and Fe elements on the surface of $MnFe_2O_4$ fibers after 5 cycles

	Mn element percentage %	Fe element percentage %
1	0.06	0.04
2	0.05	0.01
3	0.01	0.03
4	0.03	0.00
5	0.01	0.01

TG diagram that the hemp fiber treated by four different methods have three stages of mass loss. In the first stage, 50–120 °C, the fiber mass has a small range of loss. The reason is that in this temperature range, due to the endothermic precipitation of internal water and small molecules, the evaporation of water, the removal of crystal water caused by the loss of mass. It can be seen from the image that this part of the weight loss is relatively small. In the second stage, the weight loss rate of hemp is large, which is due to the decomposition of hemp fiber macromolecular chain between 300 °C and 600 °C. In the temperature range of 220 °C to 300 °C, it is due to the pyrolysis of cellulose and the cleavage of glycosidic bonds of cellulose structure.[35] As can be seen from the image, the mass loss of hemp fiber treated by different methods is very large in this temperature range, and the mass loss of hemp fiber treated by Fenton-$MnFe_2O_4$ is the largest. The degumming method was changed, and the degradation temperature was also different. The degradation temperature of hemp fiber treated by Fenton-$MnFe_2O_4$ was the highest. The increase in degradation temperature meant that the non-cellulose substances were removed and the crystallinity of the fiber was enhanced, which was consistent with the results obtained, as shown in Fig. 8(b).[36] After the third stage at 375 °C, the weight loss was due to the thermal decomposition of the cellulose component.[1,37]

As shown in Fig. 8(d), the thermal stability of hemp fibers treated with Fenton-$MnFe_2O_4$ was greatly improved compared with that of the raw hemp and hemp fiber treated by traditional alkali degumming.[38,39] Compared with the traditional Fenton degumming method, the thermal stability of hemp fiber treated with Fenton-$MnFe_2O_4$ was not reduced, and there was a slight increase. This means that Fenton-$MnFe_2O_4$ is beneficial for improving the thermal stability of the hemp fiber.

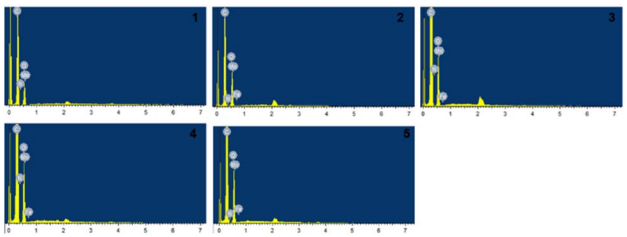

Fig. 10 EDS diagram of $MnFe_2O_4$ cycled for 5 times: (1) the $MnFe_2O_4$ hemp fiber of the first cycle; (2) the $MnFe_2O_4$ hemp fiber of the second cycle; (3) the third cycle of the $MnFe_2O_4$ hemp fiber; (4) the fourth cycle of the $MnFe_2O_4$ hemp fiber; and (5) the fifth cycle of the $MnFe_2O_4$ hemp fiber.

Effect of $MnFe_2O_4$ cycle on the properties of hemp fibers

As $MnFe_2O_4$ is magnetic, it is easy to recycle and reuse. Therefore, the optimal Fenton $MnFe_2O_4$ degumming conditions (5.3% H_2O_2 (w/w), 0.31% $FeSO_4 \cdot 7H_2O$ (w/w), and 0.045% $MnFe_2O_4$ (w/w)) were used in the above experiment. The residual gum rate was 5.74%, and the breaking strength was 18.22 cN per dtex, and the effect of $MnFe_2O_4$ cycle on hemp fiber properties was studied. After each degumming, $MnFe_2O_4$ was sucked to the bottom of the degumming solution with a magnet, and a new degumming solution was added after the degumming waste liquid was discharged. As shown in Fig. 9, the cycle of $MnFe_2O_4$ in the Fenton-$MnFe_2O_4$ system will lead to a decrease in the fiber breaking strength and an increase in the residual gum rate. This may be due to the fact that a part of $MnFe_2O_4$ is attached to the surface of the hemp fiber during the degumming process.[40] As the number of cycles increases, the amount of $MnFe_2O_4$ added decreases, which is no longer the optimal concentration, and the catalytic effect on the Fenton system is weakened, resulting in an increase in the residual gum rate. It is worth noting that when $MnFe_2O_4$ is recycled to the fourth time, the breaking strength of the fiber is relatively improved. This may be because the oxidation of the system is weakened after the fourth time, and the resin wrapped on the fiber surface increases, resulting in an increase in the breaking strength of the fiber. Theoretically, the number of cycles of $MnFe_2O_4$ is much higher than 5 times. However, in practical applications, due to the indispensable mass loss of $MnFe_2O_4$ the content of $MnFe_2O_4$ is very small at the 6th cycle, which cannot reach the catalytic effect on the system. However, we can reduce the mass loss of $MnFe_2O_4$ by centrifugation, washing and other methods to increase the number of cycles of the Fenton-$MnFe_2O_4$ system. Fig. 10 is the EDS diagram of the cycle of 5 times, and Table 8 presents the contents of Fe and Mn elements in the cycle of 5 times. As shown in Fig. 10 and Table 8, the hemp fiber treated with the Fenton-$MnFe_2O_4$ system was almost difficult to detect the two elements of Fe and Mn, indicating that the hemp fiber under this treatment was not strongly adsorbed to the metal, and the subsequent treatment will not be harmful to the human body after being made into textile products.

Conclusion

We have successfully developed a Fenton-$MnFe_2O_4$ system using $MnFe_2O_4$ to improve the Fenton system, and successfully used it

in the degumming of hemp fibers. Under the optimized degumming experimental conditions, Fenton-$MnFe_2O_4$ refining exhibited superior properties such as extremely low gum content (5.87%) and excellent breaking strength (18.22 cN per dtex). In addition, after 5 cycles of $MnFe_2O_4$, the performance of the hemp fiber still meets the needs of the spinning process, and there is still room for improvement in the number of cycles. In addition, this degumming method has the advantages of short time, less chemicals added, and no pollution to the environment, and the $MnFe_2O_4$ used can be recycled. The Fenton-$MnFe_2O_4$ process provides a new way for the removal of hemp fiber gum.

Author contributions

Chunyu Yu: investigation, writing-first draft. Yongjie Zheng: supervision, funding, acquisition, conceptualization, writing-editing. Ying Sun: analysis, writing-editing. Jiayi Wang synthesized and characterized all the samples mentioned in the manuscript. All the authors discussed the results and reviewed the manuscript.

Conflicts of interest

The authors declared no potential conflicts of interest with respect to the research, authorship and/or publication of this article.

Acknowledgements

This work was supported by the 2022 Heilongjiang Provincial Colleges and Universities Basic Scientific Research Business Fee Scientific Research Project (No. 145209510).

Notes and references

1 N. Stevulova, A. Estokova, J. Cigasova, I. Schwarzova, F. Kacik and A. Geffert, *J. Therm. Anal. Calorim.*, 2016, **128**, 1649–1660.
2 L. Pei, Z. Yu, W. Xungai and H. Christopher, *Ind. Crops Prod.*, 2021, **174**, 114158.
3 L. Cheng, S. Duan, X. Feng, K. Zheng, Q. Yang, H. Xu, W. Luo and Y. Peng, *J. Eng. Fibers Fabr.*, 2020, **15**, 155892502094010.
4 M. Yu, C. Sun, L. Wang, K. Zang, M. Li, L. Zhou and Y. Zheng, *Chem. Eng. J.*, 2021, **416**, 129122.
5 J. Zhou, Z. Li and C. Yu, *Fibers Polym.*, 2017, **18**, 1891–1897.
6 K. Liu, J. Su, J. Liang and Y. Wu, *RSC Adv.*, 2021, **11**, 28375–28380.
7 Y. Qu, W. Yin, R. Zhang, S. Zhao, L. Liu and J. Yu, *Cellulose*, 2019, **27**, 1225–1237.
8 Y. Yinzhi, F. Fangwei, X. Jinpeng, F. Kaiyang, Z. Qiang, C. Yiren, C. Xinwang and D. Zhongmin, *Polym. Bull.*, 2022, **80**, 1817–1829.
9 Q. Zhihui, Z. Shuyuan, C. Hong, M. Lijie, L. Liu, Z. Ruiyun and C. Longdi, *Ind. Crops Prod.*, 2022, **188**, 115594.
10 Y. Qu, Z. Qin, R. Zhang, D. Wu, F. Ji, Z. Shi, S. Zhao, L. Liu and J. Yu, *Carbohydr. Polym.*, 2020, **239**, 116250.
11 A. K. Sahi, M. K. Singh and A. Das, *J. Nat. Fibers*, 2021, **19**, 8842–8853.
12 Y. Shu, Y. Chongwen, Z. Bin, Z. Peihua, B. Xuerong, L. Jiawei and Z. Wenbo, *Ind. Crops Prod.*, 2022, **186**, 115189.
13 L. Pei, X. Liangjun, J. Xin, L. Xin, X. Weilin, H. Christopher and W. Xungai, *Ind. Crops Prod.*, 2022, **178**, 114620.
14 Y. Qu, S. Zhao, Z. Shi, R. Zhang, L. Liu, F. Ji and J. Yu, *Cellulose*, 2020, **27**, 4271–4285.
15 Y. Hu, Y. Li, J. He, T. Liu, K. Zhang, X. Huang, L. Kong and J. Liu, *J. Environ. Manage.*, 2018, **226**, 256–263.
16 Q. Li, A. Wang, K. Long, Z. He and R. Cha, *ACS Sustain. Chem. Eng.*, 2018, **7**, 8b04786.
17 Y. Wen, Z. Yuan, J. Qu, C. Wang and A. Wang, *ACS Sustain. Chem. Eng.*, 2020, **8**, 2688–2697.
18 B. Maryam, P. Mohammad Mehdi, D. Elnaz, D. Mohammad Javad, A. Mohsen, O. Shahriar, R. Amir, S. Mika, D. Mahdieh and A. Mohammad, *Arabian J. Chem.*, 2022, **15**, 104229.
19 X.-N. Wei and H.-L. Wang, *J. Alloys Compd.*, 2018, **763**, 844–853.
20 L. Y. Shang, S. L. Zhao, Y. W. Tian, Z. H. Zhang, S. W. Xie and P. Li, *Adv. Mater. Res.*, 2014, **881–883**, 234–237.
21 R. K. Mahajan, K. K. Vohra and V. K. Aswal, *Colloids Surf., A*, 2008, **326**, 48–52.
22 L. Gao and Z. Liu, *IEEE Trans. Magn.*, 2022, **58**, 1–7.
23 Z. Shuyuan, Q. Zhihui, Z. Ruiyun, L. Naiqiang, L. Liu, Y. Jianyong, J. Miaolei and Q. Yongshuai, *Cellulose*, 2022, **29**, 9569–9581.
24 T. M. Reineke, *Bioconjugate Chem.*, 2022, **34**, 1–2.
25 Z. Shuyuan, Q. Zhihui, Z. Ruiyun, L. Naiqiang, L. Liu, Y. Jianyong, J. Miaolei and Q. Yongshuai, *Cellulose*, 2022, **29**, 9569–9581.
26 J. Shen, X. Li and X. Yan, *ACS Omega*, 2021, **6**, 31154–31160.
27 Y. G. Thyavihalli Girijappa, S. Mavinkere Rangappa, J. Parameswaranpillai and S. Siengchin, *Frontiers in Materials*, 2019, **6**, 226.
28 F. Wu, Q. Zhang, M. Zhang, B. Sun, Z. She, M. Ge, T. Lu, X. Chu, Y. Wang, J. Wang, N. Zhou and A. Li, *ACS Appl. Mater. Interfaces*, 2020, **12**, 10142–10155.
29 N. Lu and S. Oza, *Composites, Part B*, 2013, **44**, 484–490.
30 B. Arık, O. Avinc and A. Yavas, *Cellulose*, 2018, **25**, 4841–4858.
31 G. Lin, Q. Tang, H. Huang, C. Yu, J. Yu, Z. Li and B. Ding, *Text. Res. J.*, 2022, **92**, 3579–3590.
32 H. Wang, T. Shu, P. Li, Y. Bai, M. Xiang, T. Yu, Y. Wu and L. Yu, *Text. Res. J.*, 2021, **92**, 1026–1037.
33 N. Lu and T. M. Korman, *J. Architect. Eng.*, 2012, **19**, 204–208.
34 F. Yang, Y. Ma, H. Zheng, L. Zheng and Y. Zhao, *J. Nat. Fibers*, 2019, **17**, 1401–1409.
35 W. R. Rolim, C. Lamilla, J. C. Pieretti, M. Díaz, G. R. Tortella, M. C. Diez, L. Barrientos, A. B. Seabra and O. Rubilar, *Energy, Ecol. Environ.*, 2019, **4**, 143–159.
36 L. Jun, D. Yile, M. Xiaoxiao, L. Yutong, X. Huidong, Q. Yabing and Z. Sijing, *Colloids Surf., A*, 2023, **669**, 131506.
37 M. C. Subash and P. Muthiah, *Cleaner Engineering and Technology*, 2021, **5**, 100304.
38 Q. Zhihui, Z. Shuyuan, C. Hong, M. Lijie, L. Liu, Z. Ruiyun and C. Longdi, *Ind. Crops Prod.*, 2022, **188**, 115594.
39 R. Zhu, Y. Yu, W. Yang, J. Zhao, G. Shi and J. Liu, *Text. Res. J.*, 2021, **91**, 2215–2224.
40 A. Hadi, Q. Chen, M. Curioni, R. Xiao, T. Huang and Z. Liu, *ACS Sustain. Chem. Eng.*, 2018, **6**(9), 12299–12308.